



Effect of Hooked Steel Fibers on Shear Strength of Beams Without Stirrups

Tewodros Mamo Heylemelecot ^{a*}

^aDepartment of Civil Engineering, Gafat Institute of Technology, Debretabore University, Ethiopia.

DOI:

<https://doi.org/10.20372/ajec.2023.v3.i2.897>

©2022 Kombolcha Institute of
Technology, Wollo University



ISSN : 2788-6239 (Print)

ISSN: 2788-6247 (online)

*Corresponding

Author: hmelecot21@gmail.com

ABSTRACT

This study explores the impact of incorporating hooked steel fibers on the shear strength of concrete beams. Finite element analysis was employed to analyze eighteen simply supported steel fiber-reinforced concrete beams. The investigation assesses the effects of three different fiber percentages, three shear span-to-depth ratios, and two cube compressive strengths of concrete on the shear strength of the beams. All model beams had a width of 150 mm and a depth of 250 mm. The primary variables included three fiber percentages (0%, 0.5%, and 0.75%), three shear span-to-depth ratios (1.0, 1.25, and 1.5), and two cube compressive strengths of concrete (30 MPa and 60 MPa). No shear stirrups were incorporated within the span, and the two longitudinal bars were hooked upwards behind the supports and enclosed by two stirrups at each end. To validate the finite element (FE) simulation, the study used test results available in the literature for steel fiber-reinforced concrete beams. The results from the finite element analysis were compared with the test values, demonstrating good agreement. The findings underscore the reliability of the analysis in predicting shear strength in terms of failure load and failure mode for steel fiber-reinforced concrete beams. The finite element analysis focused on eighteen simply supported steel fiber-reinforced concrete beams, primarily investigating the influence of hooked steel fibers on shear strength. The study examined the behavior of these beams, including load-deflection curves, load-ultimate shear strength curves, and shear failure modes such as diagonal cracking, ultimate shear strength, and ultimate shear load capacity. The results from the finite element analysis emphasized the significant impact of hooked steel fibers on the shear strength of concrete beams. The ultimate shear strength was observed to increase with higher concrete compressive strength, lower shear span-to-depth ratios, and increased fiber volume. Additionally, as the fiber content increased, the failure mode transitioned from shear to flexural. The influence of fiber decreased by 2.33% to 63.47% with increasing concrete compressive strength (30 MPa to 60 MPa) for shear span-to-depth ratios of 1.25 and 1.5, and decreasing shear span-to-depth ratio. **Keywords:** Shear strength, SFRC beams, Hooked steel fibres, Concrete.

1. INTRODUCTION

Steel fiber reinforced concrete (SFRC) is a composite material consisting of aggregate, Portland cement, and discrete discontinuous steel fibers. Shear failure in reinforced concrete (RC) members is a critical issue that can result in sudden failure without warning. Although shear stirrups are a common solution to minimize shear problems, SFRC can significantly increase shear strength and change the failure mode from shear to flexure [1]. In addition, SFRC can improve post-cracking strength, transfer stresses across a cracked section, and increase toughness in the hardened state [14]. The addition of fibers in a suitable fraction and geometry produces a significant increase in shear strength and can also change the failure mode from shear to flexure [7]. Also, the addition of fibers can partially stand-in transverse stirrups and it can decrease crack width, contributing to the control of concrete cracking [11]. For these reasons, fibers can significantly contribute to concrete strength when subjected to shear loads [17]. The most important properties of SFRC are its ability to improve the post-cracking strength and transfer stresses across a cracked section which increases the toughness of concrete in the hardened state [13]. Most common technical method of minimizing shear problems was providing shear stirrups [1]. A great number of studies on this topic have been conducted in the last decades using theoretical, numerical and experimental approaches [6]. They concluded that provision of shear stirrups increases the resistance to flexure-shear and diagonal tension crack formation.

However, a problem of shear behavior of reinforced concrete beams i.e., residual load carrying capacity and ductility is still an area of research [2]. In this proposed research, the steel fiber is used to replace shear stirrups [21]. These techniques were studied by many researchers using theoretical and experimental approaches [9]. However, in this study, the effects of inclusion of steel

fiber on shear strength of deep beams were studied using ABAQUS software [20]. The main objective of this study is to study the effect of inclusion of steel fibers on shear strength of concrete beams [21]. This includes investigating the effect of shear span to depth ratio on the ultimate shear strength of SFRC beams, investigating the effect of cube compressive strength on the ultimate shear strength of SFRC beams, and comparing the crack pattern and mode of failure of steel fiber with plain concrete beams [20]. This study aims to address the gap in knowledge regarding the shear behavior of SFRC beams and provide insights into the effectiveness of using hooked steel fibers as an alternative to shear stirrups.

2. MATERIAL AND METHODS

2.1 Finite element modeling

In the investigation of the shear strength of the simply supported SFRC beams, the three-dimensional ABAQUS model was developed by defining the steel fiber-reinforced concrete beams as plain concrete [21], the steel reinforcing bars including the longitudinal as well as the vertical stirrups at two ends of the beam [21], and the loads and supporting steel plates as individual sections [21]. The modeling of SFRC structures is the same as RC structures. In the proposed model, the concrete was modeled using an 8-node linear brick, reduced integration element (C3D8R) [24]. The reduced integration element was selected to decrease the simulation time as it has only one Gauss point, and fewer integration points are computed (ABAQUS 6.14-2) [24]. In terms of the steel reinforcement, the reinforcing bars, including the longitudinal and stirrup reinforcements, were modeled by a 2-node linear 3-D truss element (T3D2) [25]. The truss element in ABAQUS can be used in two or three dimensions to present a slender structural element that resists and transfers only axial forces [25]. It can also be used to model components where strain is calculated from the change in length (ABAQUS 6.14-2) [25]. The advantage of using a truss

element is that the perfect bond can easily be defined by embedding the steel bars into a host region (concrete beam) [25]. The mesh sensitivity can be eliminated if the cracks are reasonably distributed (ABAQUS 6.14-2) [25]. The appropriate mesh sizes are chosen for the model's 20mm size elements [25].

2.1.1 Model of steel fiber-reinforced concrete (SFRC) and the relationship between SFRC and reinforcement.

In the proposed research, the interaction between reinforcing bars and SFRC is assumed to have a perfect bond with each other [21]. Therefore, the interaction between concrete and reinforcement was modeled by using the embedded region option available in ABAQUS 6.14.2, which represents the perfect bond between concrete and reinforcement [24]. According to Jafarifar et al., CSC, representation of anisotropic behavior of cracking dominates modeling, while CDP uses the concept of isotropic damage in combination with tensile and compressive plasticity to define the inelastic behavior of concrete [24]. Hence, the crack opening smeared over the element length in CSC is analogous to the inelastic deformation over the element length in CDP [24]. CSC, although able to model orthotropic damage, is prone to virtual numerical stiffening and consequent instabilities in multicroaked conditions [24]. In this proposed research, CDP models were used to define a softening behavior of SFRC structures, and the numerical analyses were carried out under the displacement control method [24]. The damaged plasticity model can be used for plain concrete as well as for SFRC structures subjected to monotonic loading (displacement) under low confining pressure (ABAQUS 6.14.2) [24]. The damaged plasticity parameters include five variables that must be taken into account [24]. Some of these parameters are given a specific value in ABAQUS, whereas the others have a range between two values [24]. Two parameters have a specific value in

ABAQUS. Firstly, the hyperbolic flow potential eccentricity (ϵ), which is defined in ABAQUS as a small positive number that represents the rate at which the hyperbolic flow potential approaches its asymptote [24]. The default value given in ABAQUS for ϵ is 0.1, which is the value selected for the current model [24]. The second parameter is the ratio of SFRC strength in the biaxial state to that in the uniaxial state (f_{bo}/f_{co}) [24]. The value chosen for the proposed model is 1.16 [24]. Higher dilation angle (the internal friction angle of steel fiber-reinforced concrete) values result in more ductile behavior of concrete, whereas low values lead to brittle concrete behavior [24]. In the current model, the value of the dilation angle that gave the closest results to the normal strength plain concrete and SFRC results was 31° and 55° , respectively, as shown in Table 1 to Table 3 [24].

Table 1. The damaged plasticity parameters employed in the ABAQUS model for plain concrete (with a steel fiber volume fraction of 0%).

Dilation angle	Eccentricity	fbo /fco	Kc	Viscosity (Pa-s)
31°	0.1	1.16	0.667	0.000001

Table 2. The damaged plasticity parameters applied in the ABAQUS model for steel fiber-reinforced concrete (with a steel fiber volume fraction of 0.5%).

Dilation angle	Eccentricity	fbo /fco	Kc	Viscosity (Pa-s)
55°	0.1	1.16	0.667	0.003

Table3. he damaged plasticity parameters utilized in the ABAQUS model for steel fiber-reinforced concrete (with a steel fiber volume fraction of 0.75%).

Dilation angle	Eccentricity	fbo /fco	Kc	Viscosity (Pa-s)
550	0.1	1.16	0.667	0.0095

This value was selected through a comparison between the load deflection and the load damages results of the current model. the ratio of the second stress invariant in

tension to that in compression (K_c), the value of which must be between 0.5 and 1.0. The current default value of 0.667 given in ABAQUS was selected for the proposed model. The value selected for the proposed model is 0.003 for 0.5% of fibers and .0095 for 0.75% of fibers to reduce the simulation time. The values of the parameters required to define the plain and steel fiber reinforced concrete damaged plasticity model are shown in Table 1-3. In Tables 1 to 3, f_{bo}/f_{co} is the ratio of initial equibiaxial compressive yield stress to initial uniaxial compressive yield stress; K_c is the ratio of the second stress invariant in tension to that in compression. In the proposed ABAQUS model, the value of Poisson's ratio was equal 0.2 for plain concrete and steel fiber reinforced concrete. The equation for elastic modulus for steel fiber reinforced concrete is shown in equation 1 proposed by Padmarajaiah et al. [25]

$$E_{cf} = E_c + 2440.2 (RI) \quad \text{---- (1)}$$

Where,

RI = Fiber – reinforcing index ($RI = L_f V_f / d_f$)

V_f = Volume of fraction

L_f = Length of fiber; d_f = Diameter of fiber

The stress-strain relationship proposed by Gonzalo et al. [4] is shown in Figure 1. Like a plain concrete relationship between the stress and strain of SFRC is assumed to be approximately linear up to the ultimate stress of SFRC. The first runs from the origin of the axes to the maximum stress (curve 1 in Figure 1) and is described by the following equation.

$$\sigma^* = \frac{\alpha \epsilon^* - \epsilon^{*2}}{1 + (\alpha - 2) \epsilon^*} \quad \text{---- (2)}$$

Where, $\sigma^* = \sigma / f_{cf}$ Non-dimensional stress;

$\alpha = 1.05(E_f / f_{cf})$, Non dimensional Coefficient;

f_{cf} = Compressive strength of SFRC;

ϵ_{cf} = Critical strain;

f_{cf} = Elastic modulus of SFRC;

$\epsilon^* = \epsilon / \epsilon_{cf}$, non-dimensional strain;

The compressive strength and corresponding strain plus the elastic modulus of SFRC can be easily obtained by using the following equations:

$$f_{cf} = (1 + 4.174 \ell^* f) \quad \text{---- (3)}$$

$$\epsilon_{cf} = \epsilon_{co} (1 + 0.4823 \lambda) (V_f - 0.002606 \ell^* f) \quad \text{---- (4)}$$

Where, $\ell^* f$ is l_f / l_o non-dimensional fiber length, l_o is 30 mm Coefficient to maintain non-dimensionality, V_f is Volumetric fiber ratio, f_{co} is Compressive strength of the base concrete in MPa, determined with respect to Euro code [3]. $\epsilon_{co} = 0.0007(f_{co} / f_o)$ Critical strain of the base concrete, i.e, strain at maximum stress, f_o is 1 MPa. In the Figure 1 below the second curve (labeled as 2) is a softening branch that runs from peak stress to zero. The following parabolic equation defines the curve:

$$\sigma^* = 1 - (1/4) (1 - \sigma^*_R) (\epsilon^* - 1)^2 \quad \text{---- (5)}$$

Where, σ^*_R is the following equation of the parameters that characterize the fiber.

$$\sigma^*_R = 0.8279 + 0.3888 \ell f (35.03 \ell f - 1) < 1$$

Actually, σ^*_R is the non-dimensional stress corresponding to $\epsilon^* = 3$, as represented in Figure 3.1. This second stretch intercepts the x-axis at:

$$\epsilon^*_u = 1 + (2/\sqrt{1 - \sigma^*_R}) \quad \text{---- (6)}$$

Note: the equation for the softening part of the curve, Eq. 2.6 is only valid for SFRC with hook-ended fibers.

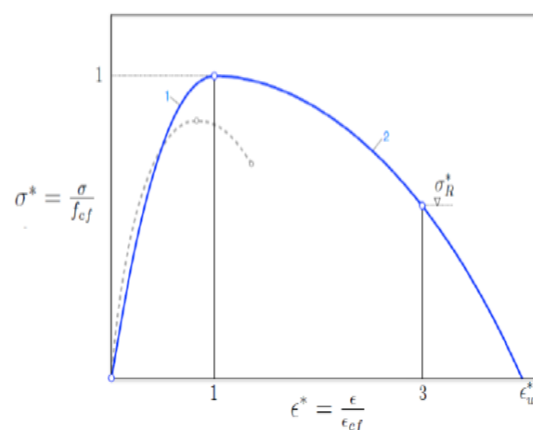


Fig 1. Illustration depicting the stress-strain relationship in steel fiber-reinforced concrete (SFRC) for structural analysis (solid curve), in contrast to the stress-strain relationship of the equivalent base concrete (broken line curve) [4]

The tensile strength of SFRC according to Figure 2 can be calculated as described below.

$$f_{ct} = 2.12 \ln(1 + f_c/10) \quad \text{---- (7)}$$

Where, f_c = cylinder compressive strength of SFRC in N/mm². In this model trilinear P.Schumacher et al, the relationship was simplified to a bilinear relationship by extending the first and third branch and calculating the intersection point, see Figure 2. The unknown intersection points were calculated with equations [25];

$$w_{int} = \frac{w_0 \cdot \frac{\sigma_{II}}{w_0 - w_2} - f_{ct}}{\frac{\sigma_{II}}{w_0 - w_2} - \frac{f_{ct} - \sigma_I}{w_1}} \quad \text{---- (8)}$$

$$\sigma_{int} = f_{ct} - \left(\frac{f_{ct} - \sigma_I}{w_1} \right) \cdot w_{int} \quad \text{---- (9)}$$

Where, w_{int} (mm) = crack width at the intersection points and σ_{int} (N/mm²) = stress at the intersection point. According to the EBCS EN 1992-1-1:2013, the stress-strain relationship of steel starts with a linear elastic ascending branch up to the yield strength followed by a linear strain hardening up to the ultimate strength.

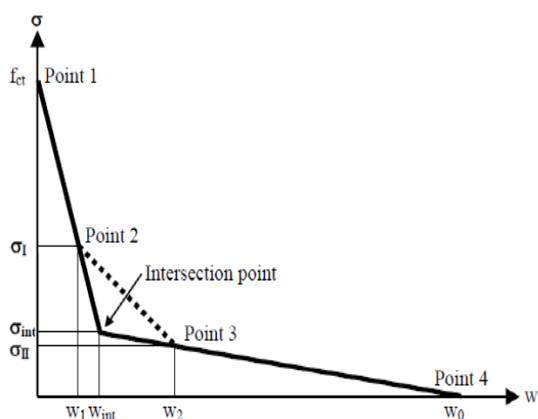


Fig 2. Softening relationship of a bilinear nature applied to SFRC beams [25]

2.2. Validation of FE model of SFRC beam under static load with test result

The static analyses presented in this section simulate the tests carried out by Yon-Keun et al., [23] are used. These static beams have been modeled by ABAQUS software using the FE method and the analyses results are compared with the test results. The three beams, 0,

0.5 and 0.75 percentages of steel fibers reinforced concrete with shear span to depth ratio 2, specimens used in this research, identified as FHB1-2, FHB2-2 and FHB3-2, were designed according to the empirical equation defined by different investigators.

Figure 3 shows the details of test beams. All of the beams had identical cross-sectional dimensions (125mm*250mm), effective depths (212 mm), and flexural reinforcement (two D16 bars). The longitudinal bars were hooked upwards behind the supports and enclosed by three D10 stirrups at each end. No stirrups were included within the shear span. The test beams were supported by a roller on one end and a hinge at the other end. Two equal loads were applied to the beam using a steel spreader and 80mm-wide x 40mm-thick loading plates.

The water-cement ratio (w/c) was 0.33 for all higher-strength beams and 0.62 for the normal strength beams. Type I Portland cement was used for concrete and the maximum crushed aggregate size was 19 mm. The steel fibers were hooked, 50mm long, and 0.8 mm in diameter. The flexural yield stress, ultimate strength and nominal yield strength of fibers were 442 MPa, 638 MPa and 1079 Mpa respectively.

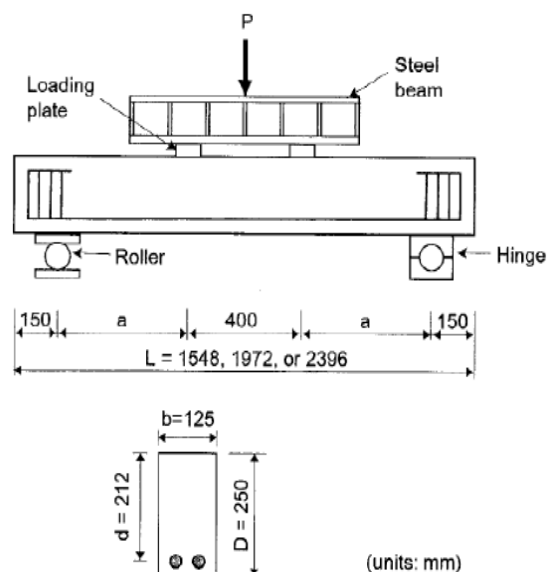


Fig 3. Information regarding the test beams [23]

The support and load have been applied on beam by circular discrete rigid plate with d of 100 mm. Surface to surface (Explicit) contact method has been used to model the contact behavior between SFRC beam and steel support/load plates. The element size of 20 mm for concrete beam, reinforcement and steel support plate has been proved the most reasonable element size from mesh sensibility analysis. The constitutive material property of SFRC has been modeled by the CDP model of ABAQUS. The beam has been modeled with full scale to ensure the actual behavior of the test.

2.2.1 Load-displacement plot for FHB1-2 beam with 0 % fiber content.

Figure 4 shows the load versus displacement behavior of the beam FHB1-2. The load-displacement of FHB1-2 has been found by FE analysis to be similar to the actual result viewed in the test. ABAQUS modeled the beam to be almost similar to the actual result.

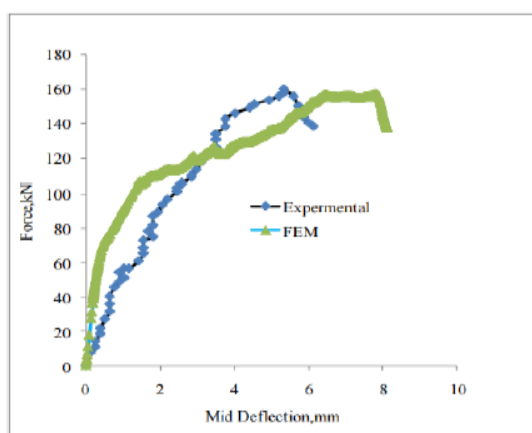


Fig 4. Comparison between the reaction force and displacement diagram of the FHB1-2 beam analyzed numerically and the results obtained from the study [23]

2.2.2 Load-displacement curve for the FHB2-2 steel fiber-reinforced concrete (SFRC) beam containing 0.5% of fibers.

FHB2-2 SFRC beam with test result found by Yon-Keun et al., [23] are shown in Figure 5. It shows the load vs. Displacement behavior of FHB2-2 SFRC beam as predicted by the FE analysis with the test result. Up to

the yielding of longitudinal reinforcement, the predicted value of FHB2-2 has been found to be very similar to the actual result observed in the test. The yielding point and displacement of the beam has been estimated well by the ABAQUS model.

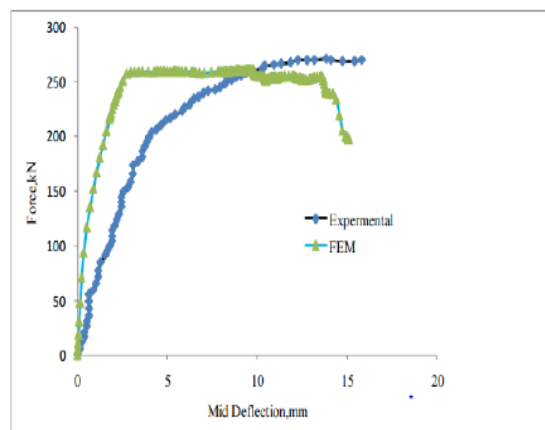


Fig 5. Comparison of the reaction force versus displacement diagram from the numerical analysis

2.2.3 Load-displacement curve for the FHB3-2 steel fiber-reinforced concrete (SFRC) beam with 0.75% fiber content

Figure 6 shows the load vs. displacement behavior of FHB3-2 SFRC beam as predicted by the FE analysis along with the test result. Up to the yielding of longitudinal reinforcement, the predicted value of FHB3-2 has been found to be very similar to the actual result observed in the test.

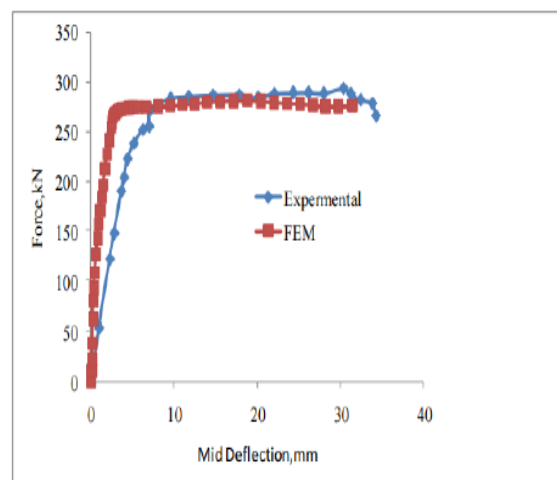


Fig 6. Comparison of reaction force vs displacement diagram of numerically analyzed FHB3-2 SFRC beam with test result found by [23]

2.2.4 Load-displacement curve for the FHB3-2 steel fiber-reinforced concrete (SFRC) beam with a fiber content of 0.75% .

The beam failed abruptly along a single shear crack. In specimen FHB1-2, without steel fibers, initial flexural cracks appeared near the midspan, eventually leading to shear cracks within the constant shear regions.

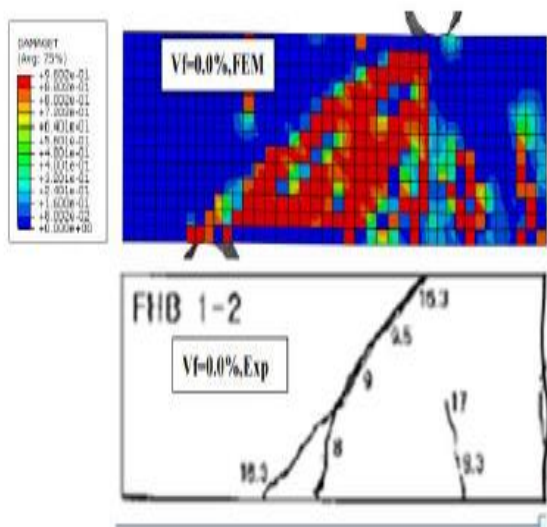


Fig 7. Failure modes observed in the FHB1-2 beam test results and the results obtained from finite element analysis.

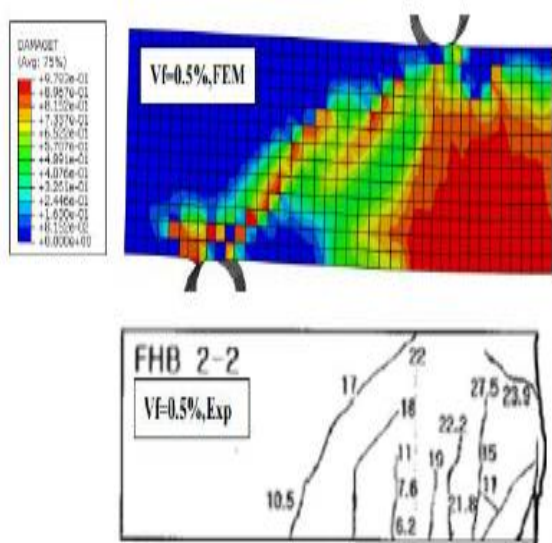


Fig 8. Failure modes observed in the FHB2-2 beam based on both test results and finite element analysis results.

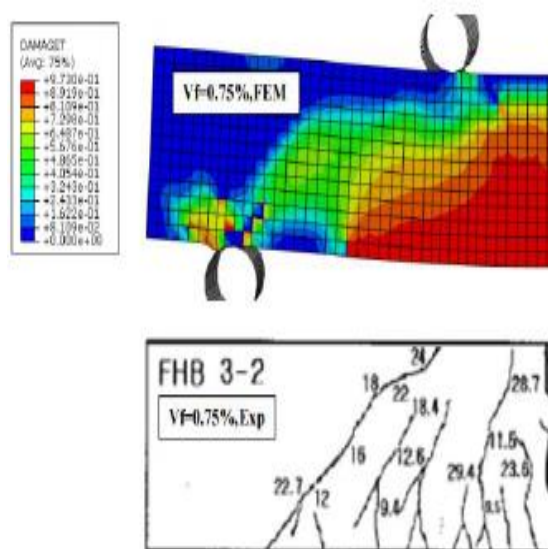


Fig 9. Failure modes observed in the FHB3-2 beam based on both test results and finite element analysis results.

As the steel fiber volume increased to 0.50% and 0.75% for specimens FHB2-2 and FHB3-2, respectively, the failure mode transitioned to a combination of shear and flexure. In these specimens, significant diagonal shear cracks and vertical flexural cracks formed, potentially contributing to the failure. With the increasing volume of steel fibers, shear and flexural cracks became closely spaced. The failure modes of the FHB1-2 beam are illustrated in Figures 7 to 9.

3. RESULTS AND DISCUSSION

3.1 General failure modes and crack development

The inclusion of steel fibers in the concrete greatly affected the observed tension cracking patterns, which are shown in Figure 10 for three beams with $a/d=1$ and C30. The three beams are identical in dimension and parameter except for the addition of steel fibers. As shown in the Figure 10, beams without steel fibers, the mode of failure of a beam is shear. While a mode of failure of a beam with 0.5% and 0.75% of fibers changed to a combination of shear and failure, and pure shear, respectively. As the shear span to depth ratio increased to 1.25 and 1.5 for beam without fibers, the failure mode gradually changed to combine shear-flexure. The reason is

arching action becomes less effective with increasing a/d . The eighteen beams were modeled in this paper to illustrate the effect of adding steel fibers to concrete beams. Of the twelve beams that contained steel fibers, only one failed in combination of shear and flexure.

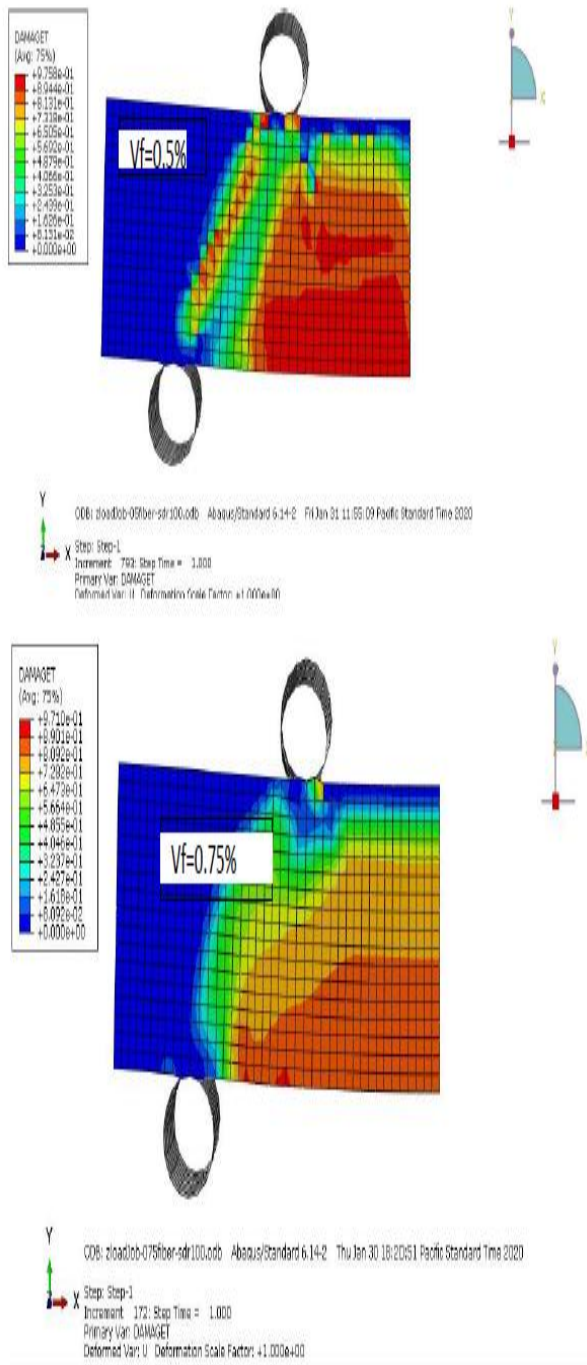


Fig 10. Crack patterns under tension and the failure mode for beams with concrete strength C30 and a/d ratio of 1

3.2 Ultimate shear load behaviors

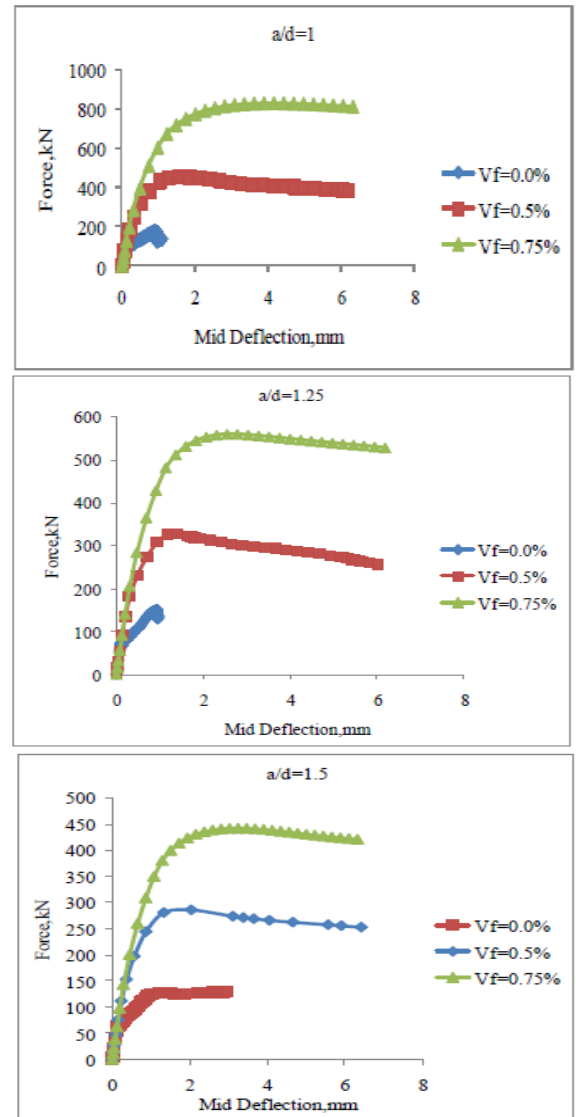


Fig 11. The influence of steel fiber volume fraction on the ultimate shear load of SFRC beams with C30 concrete at a/d ratios of 1, 1.25, and a

Typical load-mid deflection responses of the plain and hooked end steel fiber reinforced concrete (SFRC) beams with concrete strength of C30 and C60 at a/d of 1, 1.25 and 1.5 are shown in Figure 11. It shows that failure in the plain beam was sudden, immediately after attaining the peak load and could not be controlled even in displacement control. The response of the SFRC beams is a linear relationship up to peak load like that load response of the plain beams.

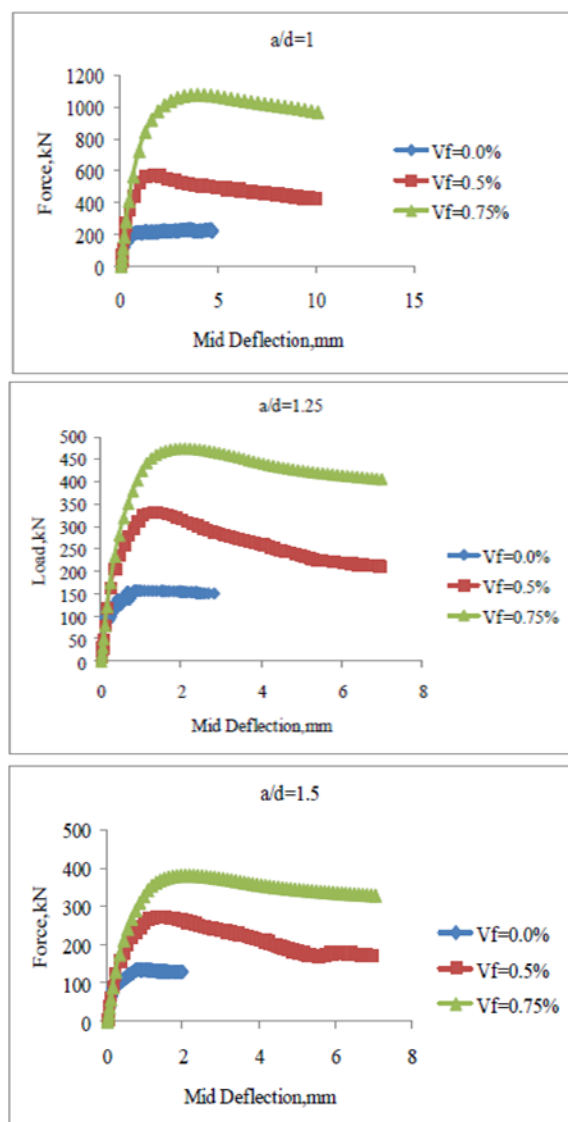


Fig 12. Effect of steel fiber volume fraction on ultimate shear load of SFRC beams with ($a/d=1, 1.25$ and 1.5) for C60

After the peak load there is a continuous decrease in the load carrying capacity with increasing deflection following which, the load carrying capacity essentially levels to a constant value with increasing deflection. In the 0.5% and 0.75% SFRC beams, there is a large increase in the shear capacity when compared to the plain concrete beams (without steel fibers). After the first shear diagonal crack appeared, the plain deep beam stiffness decreased significantly. However, the stiffness of the SFRC deep beams decreased slowly as shown in Figure

11. No significant stiffness reduction was observed after the formation of the cracks. The reason for the increase in stiffness is that steel fiber increases the elastic modulus of concrete and the tensile stiffness. However, the effect of steel fiber on the elastic modulus is small as shown in Figure 11. In addition, the steel fiber significantly increased the corresponding deflections when the beam without stirrups reached its ultimate load and failure. These behaviors were typical of the other remaining beams. As shown in Figure 11, the influence of steel fiber on shear capacity decreases as it increases the shear span to depth ratio. For example the effect of steel fiber on a beam with C30 at $a/d=1$ and $a/d=1.5$, the effect of inclusion of 0.5% of steel fiber increased 161.97% and 122.75% of shear capacity of beam with $a/d=1$ and $a/d=1.5$, respectively. The effect of inclusion of steel fiber can be varying when the compressive strength of concrete increases as shown in the Figure 12. For SFRC beams with concrete compressive strength C60 have higher shear capacity than SFRC beam with concrete compressive strength C30.

3.3 Influence of the shear span to depth ratio on the ultimate shear strength

The ultimate shear strength is defined as the strength at which the failure loads of the beam in a shear situation. The shear span to depth ratio defines the type of member, which be governed either by arch action or beam action. In this thesis, all the beams analyzed are deep beams. The ultimate shear strengths of eighteen beams. for two cube strengths of concrete (C30 & C60) respectively , in terms of the ultimate stress at failure , which is defined as the maximum shear force, which is extracted from FE, divided by the beam width (b) and effective depth (d). Figure 13 shows that the ultimate shear stress decreases with increasing a/d under different fiber volume of fraction. In addition, ultimate shear stress of the beams with a/d of 1.0 is significantly large in comparison to those with a/d of 1.5 which can be at-

tributed to the fact that arching action becomes less effective with increasing a/d . Similarly, Figure 13 shows that the ultimate shear stress appreciably increased with increasing a/d .

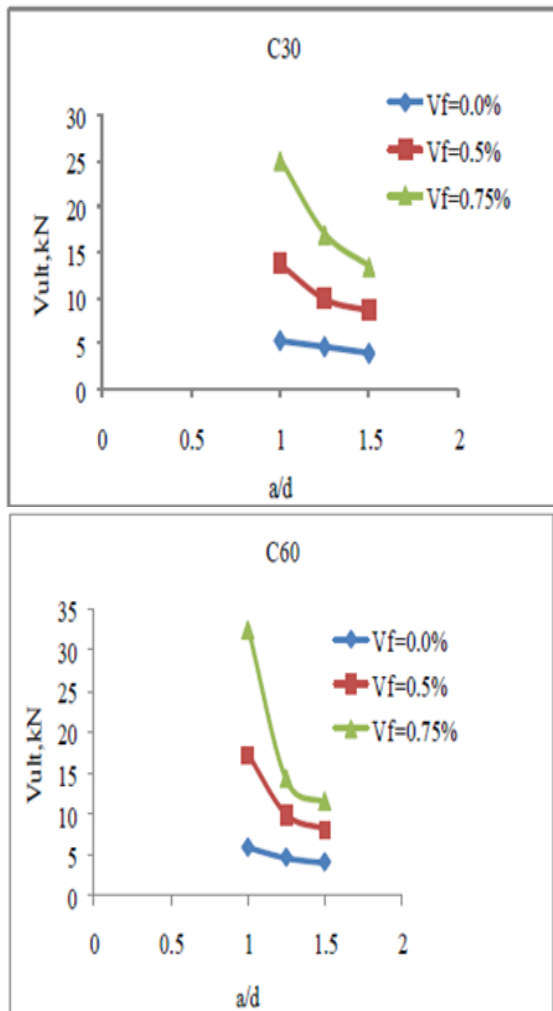


Fig 13. Impact of the shear span to depth ratio (a/d) on the ultimate shear stress for C30 and C60 beams with various fiber volume fractions.

However, ultimate shear stress of the beams for C30 with $a/d=1.0$ is significantly larger compared with beams C60 under the same a/d value. One of the limitations is that the study only investigated the effect of steel fiber on the behavior of deep beams with a/d ratio of 1, 1.25 and 1.5 and two concrete strengths of C30 and C60. Future research could extend the study to investigate the effect of steel fiber on other types of concrete

members such as slabs, columns, and walls, and consider a wider range of concrete strengths.

3.4 Influence of fiber volume fraction on ultimate shear strength

Figure 14 shows the influence of fiber volume fraction on the ultimate shear strength of different SFRC beams with $a/d=1.0, 1.25,$ and 1.5 [20]. For beams ($a/d=1$), it can be seen from Figure 14 that shear strength marginally increases as the volume of fiber increases to a certain value (about 0.5%), after which shear strength increases drastically for concrete strength C30 [20]. However, for beams with $a/d=1.5$, little improvement of shear strength with an increasing volume of fiber was observed [20]. It is worth noting that a similar behavior for SFRC beams was reported by Cucchiara et al., 2004 [20].

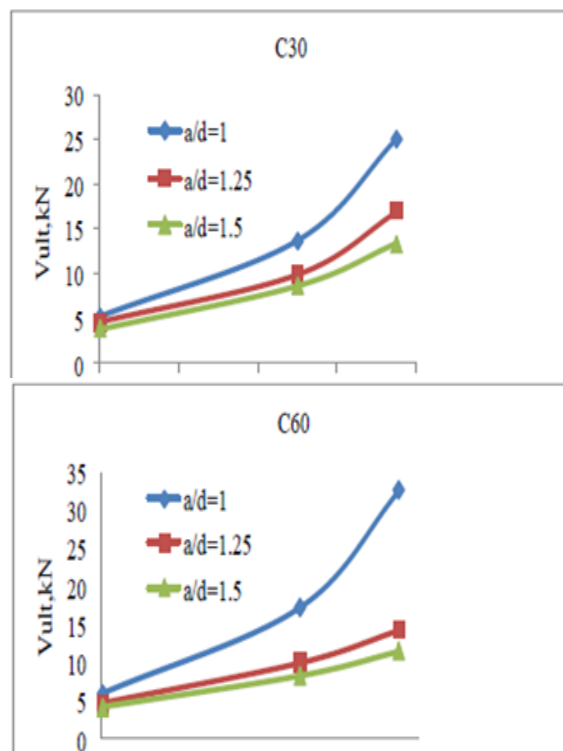


Fig 14. Effect of steel fiber volume content on the ultimate shear strength of sfrc beams without shear stirrups in C30 and C60 concrete

Table 4. Summary of the outcomes for simulated beams

Beam ID	a/d	Vol- ume of fi-	Ultimate load(kN)		Mid deflection(mm)		Comparison of Ultimate load(%)		Failure mode	
			C30	C60	C30	C60	C30	C60	C30	C60
A1-F0	1	0.0	173.08	195.06	0.916	0.58	0	0	hear	Shear
A1-F5		0.5	453.43	569.51	1.557	1.64	161.97	191.96	Shear flexure	flexure
A1-F75		0.75	0.75	829.26	1077.8	4.160	3.91	379.11	452.54	Flexure
A2-F20	1.25	0.0	151.48	154.57	0.919	0.65	0	0	shear	Shear - compression
A2-F5		0.5	327.34	330.41	1.407	1.27	116.09	113.76	Flexure	Flexure`
A2-F75		0.75	559.83	473.15	2.551	2.08	269.57	206.10	Flexure	Flexure
A3-F0	1.5	0.0	128.57	135.40	1.400	0.78	0	0	Shear-ten- sion	Shear - tension
A3-F5		0.5	286.39	273.42	2.038	1.40	122.75	101.93	Flexure	Flexure
A3-F75		0.75	441.48	381.17	3.249	2.16	243.37	181.51	Flexure	Flexure

For example, increase in the volume of fraction of steel fibers with 0.5% and 0.75% increased the ultimate shear strength of SFRC beams with C30 and $a/d=1.0$ by 161.97% and 379.11%, respectively. In addition, Figure 14 shows that the ultimate shear strength of the beams with $a/d=1.0$ and C60 is appreciably large in comparison to those with a/d of 1.5 for 0.75% of fiber volume fraction. The effectiveness of fiber decreases as compressive strength increases.

3.4 Impact of cubic concrete strength

The compressive strength of concrete is the commonly used property to relate with the shear capacity of concrete. The result obtained as shown in Table 4 generally, increase in compressive strength increases the ultimate shear strength of concrete. However, the influence of steel fibers on shear strength of SFRC beams with $a/d=1.25$ and 1.5 decreases with increasing concrete

strength. But, for SFRC beams with $a/d=1$, the effect of fibers were increased when the compressive strength of concrete increased. For example, when the compressive strength of concrete increased from 30 to 60 MPa, shear capacity of SFRC beams with $a/d=1.25$ and 1.5 decreased by 2.33% to 63.47%. Similarly, mid deflection which is corresponding to maximum shear capacity decreases as cube compressive strength increases.

3.5 Influence of steel fiber on shear ductility

The shear ductility can measure the ductility of beams failing in shear. The relationship between mid-deflection and fiber volume fraction is illustrated in Figure 3.7. Generally, the shear ductility increases as the volume of fiber increases. The effect of steel fibers on shear on $a/d=1$ than $a/d=1.25$ and 1.5. As the steel fiber volume fraction increased from 0.0% to 0.5% for beams with $a/d=1$ and 1.25, the effect of fiber was not significant when compared with beams with $a/d=1$.

4. CONCLUSION

The Finite Element (FE) results elucidate the substantial impact of hooked steel fibers on the shear strength of concrete beams. Based on the current investigation, the following conclusions can be drawn:

There is a noteworthy enhancement in the ultimate shear strength of deep Steel Fiber Reinforced Concrete (SFRC) beams with an increase in fiber content. The study reveals an up to 452.54% improvement in the ultimate shear strength of SFRC beams when the volume fraction of steel fiber is increased from 0.5% to 0.75%. The ultimate shear strength also shows an increase with the rise in concrete compressive strength. However, for SFRC beams with a shear span to depth ratio (a/d) of 1.25 and 1.5%, the influence of steel fibers on shear strength decreases by 2.33% to 63.47% as the cube compressive strength of concrete increases from C30 to C60. Additionally, the ultimate shear strength experiences a decrease with the increase in shear span to depth ratio. The effect of fibers diminishes with increasing concrete compressive strength and decreasing a/d . Generally, shear ductility improves as the volume of steel fiber increases. This effect is more pronounced for $a/d=1$ compared to $a/d=1.25$ and 1.5. The incorporation of steel fibers in fabricating SFRC deep beams alters their failure modes. With an increase in fiber content, the failure mode transitions from brittle shear to ductile flexure mode. This transition is attributed to the fibers enhancing shear strength by providing post-cracking diagonal tension resistance. Moreover, the fibers contribute to improved cracking distribution, akin to the effect of stirrups, resulting in reduced crack widths and an increase in shear resistance through aggregate interlock.

REFERENCES

- [1] ACI-ASCE, "Recent approaches to shear design of structural concrete", American Society of Civil Engineers, 1973.
- [2] S.A Ashour, G.S Hasanain, F.F.Wafa, "Shear behavior of high strength fiber reinforced concrete beams", ACI Structural Journal, 1992.
- [3] Eurocode, "Design of concrete structures - General rules and regulations for buildings", Part 1-1, London: British standards Institution, 2004.
- [4] Gonzalo Ruiz, Angel de la Rosa, S. Ebastien Wolf and Elisa Poveda, "Model for the compressive stress-strain relationship of steel fiber-reinforced concrete for non-linear structural analysis", ACI, 2018.
- [5] M.Imam, L.Vandewalle, and F.Mortelmans, "Shear capacity of steel fiber high-strength concrete beams", American Concrete Institute, pp. 227-241, 1994.
- [6] N. John Karadelis and Lei Zhang, "On the numerical simulation of steel fiber reinforced concrete", Journal of Civil Engineering Research, pp. 151-157, 2015.
- [7] M. Khuntia, B.Stojadinovi, S.C.Goel, "Shear strength of normal and high strength fiber reinforced concrete beams without stirrups", ACI Structural Journal, 1999.
- [8] Y.K.Kwak, M.Eberhard, W.O.Kim and J.S.Kim, "Shear strength of steel fiber-reinforced concrete beams without stirrups", ACI Structural Journal, pp. 530-538, 2002.
- [9] R. Londhe, "Experimental investigation on shear strength of sfrc beams reinforced with longitudinal tension steel rebar", Asian Journal of Civil Engineering, pp. 385- 395, 2010.
- [10] J.Mac Gregor, "Reinforced concrete; Mechanics and design", Englewood Cliffs, New Jersey, 1992.
- [11] M.A.Mansur, K.C.G. Ong, P. Paramasiva, "Shear strength of fibrous concrete beams without stirrups", ASCE, 1986.
- [12] Morsch Der Eisenbetonbau, "Concrete-Steel construction", Engineering News Publishing, 1909.

- [13] N. Jafarifar, K. Pilakoutas, H. Angelakopoulos, T. Bennett, "Post-cracking tensile behavior of steel-fiber-reinforced roller-compacted-concrete for FE modelling and design purposes", *Materials De Construction*, 2017.
- [14] R.Narayanan and I.Y.S Darawish, "Use of steel fibers as shear reinforcement", *ACI Structural Journal*, pp. 216-227, 1987.
- [15] R.Narayanan, and I.Y.S. Darwish, "Fiber concrete deep beams in shear", *ACI Structural Journal*, pp. 141-149, 1988.
- [16] E.A. Paulay, "Horizontal construction joints are cast in place of reinforced concrete", *ACI Special Publication*, pp. 599-616, 1974.
- [17] A.Sharma, "Shear strength of steel fiber reinforced concrete beams", *ACI Journal*, pp 624-628. 1986.
- [18] T.Soetens, "Design models for the shear strength of prestressed precast steel fiber reinforced concrete girders", *Magnel Laboratory for Concrete Research*, 2015.
- [19] J. Struct, "Solids influence of fiber properties on shear failure of steel fiber reinforced beams without web reinforcement: ANN modeling", *Latin American journal of solids and structures*, 2016.
- [20] M.A.Tantary, "prediction of shear strength of steel fibre based concrete beams without shear stirrups", *IJRTE*, pp.1930-1937, 2019.
- [21] V.T. Babar, P.K. Joshi and D.N. Shinde. "Shear strength of steel fiber reinforced concrete beam without stirrups", *International Journal of Advanced Engineering Technology*, 2015.
- [22] J. Walraven, "Mechanisms of shear transfer in cracks in concrete - A survey of literature", *Stevin Laboratory; Delft University of Technology*, 1978.
- [23] Yoon-Keun Kwak, Marc O. Eberhard, Woo Kim, and Jubum Kim "Shear strength of steel fiber-reinforced concrete beams without stirrups", *ACI*, 2003.
- [24] N.Jafarifar, K.Pilakoutas, H.Angelakopoulos, "Post-cracking tensile behaviour of steel-fibre-reinforced roller-compacted-concrete for FE modelling and design purposes", *Materials de Construction*, vol.67, issue 326, p. 122, ISSN 0465-2746, 2017.
- [25] S.K. Padmarajaiah, "Flexural strength predictions of steel fiber reinforced high-strength concrete in fully/partially prestressed beam specimens", *Cement and Concrete Composites*, vol. 26, issue 4, pp. 275-290, 1999.
- [26] P. Schumacher, "Bond of reinforcing bars in self-compacting steel fiber reinforced concrete", *Conference, Bond in Concrete, Budapest, Hungary* pp. 823-830, 2002.